Journal of Thermal Analysis and Calorimetry, Vol. 70 (2002) 371–378

SPECIFIC HEAT STUDY OF THE COMPLEX PHASE TRANSITIONS IN MAGNETISM AND DIELECTRICITY ON TRIANGULAR LATTICE ANTIFERROMAGNETS*

K.Yamanaka[1], *Y. Nishiwaki*[1], *K. Iio*[1**], *T. Kato*[2] *T. Mitsui*[2], *T. Tojo*[4] *and T. Atake*[4]

[1]Department of Physics (Cond. Mat. Phys.), Graduate School of Science and Engineering, Tokyo Institute of Technology, 2-12-1 Oh-okayama, Meguro-ku, Tokyo 152-8551, Japan
[2]Department of Physics, Faculty of Education, Chiba University Yayoi-cho, Inage-ku, Chiba 263-8552, Japan
[3]Faculty of Pharmaceutical Science, Teikyo University, Sagamiko, Kanagawa, 199-0106 Japan
[4]Materials and Structures Laboratory, Tokyo Institute of Technology, 4259 Nagatsuta-cho, Midori-ku, Yokohama, 226-8503 Japan

Abstract

The complex phase transitions involving dielectricity and magnetism on distorted triangular lattice antiferromagnets, '$KNiCl_3$-family' crystals, which have the crystal structures derived from the prototype $CsNiCl_3$, were studied through the heat capacity measurements. These crystals are classified into characteristic three groups from the viewpoint of magnetic and structural properties clarified so far. The results of the dielectric constant measurement as a function of temperature are also presented in detail. The present calorimetric study reveaed that the structural successive phase transitions rather than the magnetic transitions in these crystals are recognized more distinctly as the presence of specific heat anomalies at the respective phase transition points.

Keywords: complex phase transition, distorted triangular lattice antiferromagnet, heat capacity measurement, spin frustration

Introduction

Compounds of the ABX_3-type generic chemical formula, where A, B and X are an alkali, 3d-transition metal and oxygen or halogen, take various kinds of crystal structure characterized by the stacking of closed-packed AX_3 layers. The packing types of c-c-c and h-h-c on a cubic and a hexagonal $BaTiO_3$, respectively, have been well known to exhibit ferroelectricity and successive structural phase transitions. Another packing type of h-h-h on the typical hexagonal structure of $CsNiCl_3$-type, where

* This paper was presented at the Second International Symposium on the New Frontiers of Thermal studies of Materials, Yokohama, Japan, November, 2001.

** Author for correspondence: E-mail: iio@lee.cme.phys.titech.ac.jp

1418–2874/2002/ $ 5.00
© 2002 Akadémiai Kiadó, Budapest
Akadémiai Kiadó, Budapest
Kluwer Academic Publishers, Dordrecht

$–BX_3–$ linear chains of infinitely connected face-shared BX_6 octahedral run along the crystal *c* axis, yields interesting magnetic properties ascribable to an arrangement of magnetic *B* ions along the chains and to that on the triangular lattice in the *c* plane. In the case where the magnetic exchange interactions between *B* ions are antiferromagnetic, these compounds are generally treated as the quasi-one-dimensional system along the *c* axis and as the triangular lattice antiferromagnets possessing geometrical spin frustration in the *c* plane [1].

For the hexagonal ABX_3-type compounds, the spin frustration and its releasing effect as a counter part are intrinsic problems of physical interest. In order to clarify the effect of frustration cancellation upon the magnetic phase transition and the critical behavior of the triangular antiferromagnets, the present authors have been studied the magnetic properties and the magnetic structures stabilized at low temperatures for so-called '$KNiCl_3$-family' crystals, where the spin frustrations can be released partially owing to a slight lattice distortion accompanied with structural transitions. Hence, the several novel properties involving dielectricity and magnetism were observed in these crystals, such as the coexistence of antiferromagnetism and ferroelectricity, or the presence of dielectric anomaly around magnetic ordering.

$KNiCl_3$ has been known as a typical crystal for the distorted system descended from the prototype $CsNiCl_3$ (we designate it as the hexagonal perovskite structure with $P6_3/mmc$), where the room temperature (RT-) structure of $KNiCl_3$ was firstly reported [2]. The space group of this structure is the non-centrosymmetric $P6_3cm$ with $a\sqrt{3}\cdot a\sqrt{3}\cdot c$ unit cells, where $–(NiCl_3)^-–$ chains slightly shifted along the linear chain parallel to the *c* axis in an up-up-down alignment. This distortion was triggered by softening of the K_4 mode lattice vibration with the wave vector described by the *K* point of the reciprocal lattice of the prototype structure [3]. We call the crystal which is isomorphic or quasi-isomorphic to RT-$KNiCl_3$ at certain temperatures a member of the $KNiCl_3$-family. At this stage $KNiCl_3$ [4] itself, $RbMnBr_3$ [5], $TlFeCl_3$ [6], $RbFeBr_3$ [7], $RbCoBr_3$ [8] and $RbVBr_3$ [9] are acknowledged as members of their family. According to their magnetic, dielectric and structural properties, the $KNiCl_3$-family crystals can be classified into following three groups. Group I compounds ($KNiCl_3$, $RbMnBr_3$ and $TlFeCl_3$) undergo successive structural phase transitions at temperatures higher than their magnetic ordering points. Ferroelectricity were observed at structurally intermediate phases and vanished in the lowest-temperature phase. Group II compound ($RbFeBr_3$) exhibits both ferroelectricity and antiferromagnetism with weak-ferromagnet moment [10], thus is described as ferroelectromagnets [11] at the lowest-temperature phase. The dielectric Curie point (39.5 K) is rather higher than the magnetic successive Néel points (5.5 and 2.0 K). Group III compounds ($RbCoBr_3$ and $RbVBr_3$) show dielectric anomalies around magnetic ordering temperature region. In particular, $RbCoBr_3$ shows a simultaneous phase transition of ferroelectricity and antiferroelectricity at 37.0 K.

In order to clarify these successive structural and magnetic phase transitions, the experimental measurements are required from the aspects of complex system of magnetism and dielectricity. The present heat capacity study of revealing specific heat

anomalies due to both contributions will provide helpful information on the complex phase transitions.

Experimental

Single crystals of $KNiCl_3$-family were grown by the vertical Bridgman method in the evacuated quartz tubes from a melt of equimolar mixture of AX and BX_2.

Samples for the measurements of dielectric constants were cut from single crystal lump with a knife, and shaved as a thin plate of the c plane or cleaved as a thin plate of the ac plane. Silver paste was used for electrodes. The electric capacity C of a sample was measured at a frequency range from 10 kHz to 1 MHz and in a temperature range from 4.2 to 300 K with using a low-frequency impedance analyzer (YHP 4192A). In this paper the data at 1 MHz are shown for convenience sake. The 50 Hz D–E hysteresis loops, to check the polarity of the samples, were observed by use of the conventional Sawyer–Tower circuit at temperatures from 15 K to the room temperature. Observed loops were recorded with a digitizing oscilloscope (Tektronix TDS420) and photographed images were digitally processed. To check the effects of structural changes on magnetic properties, the magnetic measurements were carried out with a Quantum Design Co. MPMS XL SQUID system in a temperature range from 2.0 to room temperature.

Heat capacities were measured by the relaxation method using Quantum Design PPMS heat capacity measurement module for $TlFeCl_3$ and $RbFeBr_3$, or by the adiabatic calorimetry method using laboratory-made calorimeter (Atake lab. Materials and Structures Laboratory of Tokyo Inst. Tech.) for $RbCoBr_3$.

Results and discussion

The structural phase transition points of the $KNiCl_3$-family crystals, which are determined from previous dielectric, magnetic, optical and the present heat capacity measurements, are listed in Table 1. The structural and magnetic properties including the sequence of successive transitions are quite similar for the crystals in each category. Detailed experimental studies of $TlFeCl_3$ (representing the Group I), $RbFeBr_3$ (Group II) and $RbCoBr_3$ (Group III) are discussed in the following sections.

$TlFeCl_3$ (Group I)

The crystals belonging to Group I commonly undergo the successive structural phase transitions, and show characteristic dielectric behavior along the crystal c axis; Fig. 1a is for the case of $TlFeCl_3$, though the other member of the Group I show similar dielectric behavior as $TlFeCl_3$'s. [4, 5]. The data on ε_c (T) in heating and cooling runs indicate that the transitions at T_{st2} (179 K) and T_{st3} (83 K) are the second-order and the transition at T_{st4} (79 K) with an obvious thermal hysteresis is the first-order one. On the contrary, $\varepsilon_{ac}(T)$ curve does not exhibit observable anomalies. As shown in the previous reports, the ferroelectric D-E loops were clearly observed at phases II

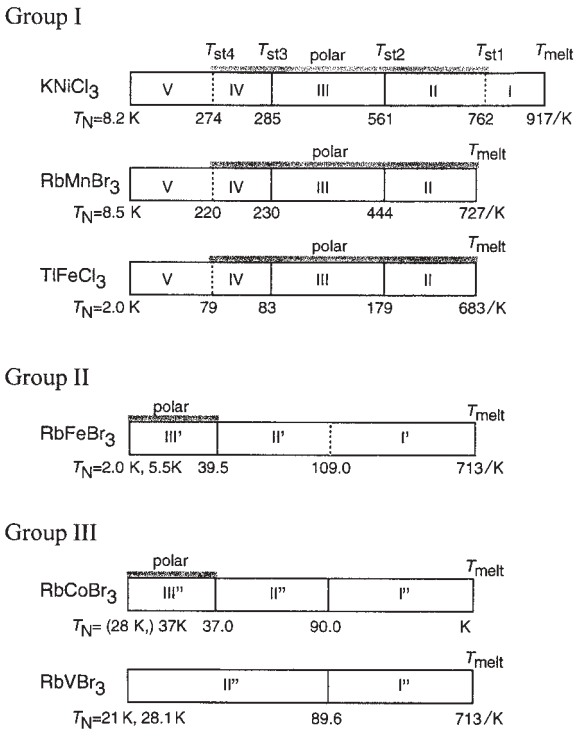

Table 1 The list of the successive phase transitions for three Groups of $KNiCl_3$-family crystals; the roman numbers in each phase indicate corresponding structural phases. The first-order and second-order transitions are shown as dotted and solid lines in table, respectively

and IV, and quite small hysteresis loops were observed at phases III. Therefore, the crystals of Group I are recognized as polar at phase II, III and IV.

The molar heat capacities measured at temperatures from 2.0 to 200 K by the relaxation method are plotted in Fig. 1b; all measurement was performed after cooling from room temperature to 2 K, at the rate of 3 K min^{-1} in a heating run. The second-order phase transition at T_{st2} indicating structural change from $P6_3cm$ at phase III to $P6_3mc$ at phase II, can be recognized as a small hump in the normal heat capacity curve. However, the two successive structural phase transitions at T_{st4} and T_{st3} are hardly observable in the normal heat capacities, hence, the Debye characteristic temperatures corresponding to the measured heat capacities around T_{st3} and T_{st4} assuming 15 degrees of freedom are shown in an inset figure of Fig. 1b. Deviations from the assumed normal base line were slightly recognized at T_{st3} and T_{st4}, though the curve of $\varepsilon_c(T)$ showed obvious anomalies at the corresponding temperatures. Meanwhile, small but distinctive undefined anomaly is recognized in the curve of C_p/T *vs.* T at

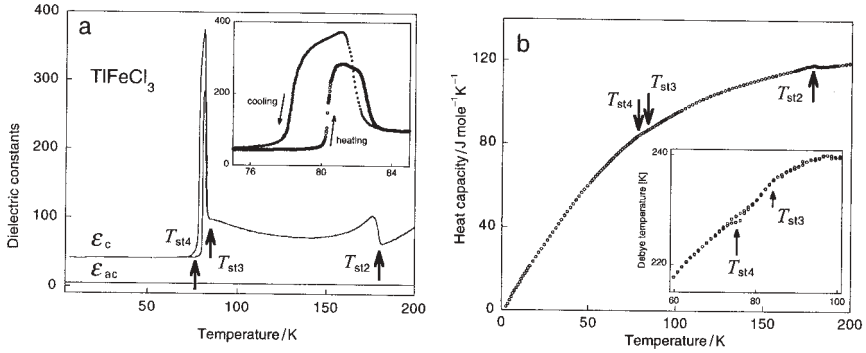

Fig. 1 The temperature dependence of dielectric constants $\varepsilon_c(T)$ and $\varepsilon_{ac}(T)$ of $TlFeCl_3$ (Group I) at 1 MHz. The inset shows the behavior of $\varepsilon_c(T)$ in cooling and heating runs around T_{st3} and T_{st4}. The thermal hysteresis is only observed around T_{st4} (a); The temperature dependence of molar heat capacity of $TlFeCl_3$. The inset figure means the Debye characteristic temperatures corresponding to the measured heat capacities around T_{st2} (b)

20 K; its origin is not determined yet. The excess heat capacities around T_{st2} due to the phase transition are obtained by subtracting the normal base line estimated with fiiting smoothly from the measured heat capacities as shown in Fig. 2.

$RbFeBr_3$ (Group II)

The Group II is only assigned for $RbFeBr_3$ which also undergoes successive structural phase transitions at T_{st1} (109.0 K) and T_{st2} (39.5 K) [7]. The dielectric constants for *c* and *ac* plane are shown in Fig. 3a. The divergence of $\varepsilon_c(T)$ is a clear indication of the ferroelectric-paraelectric phase transition. The spontaneous polarization along the *c* axis decreases normally with increasing temperature and disappears at T_{st2}.

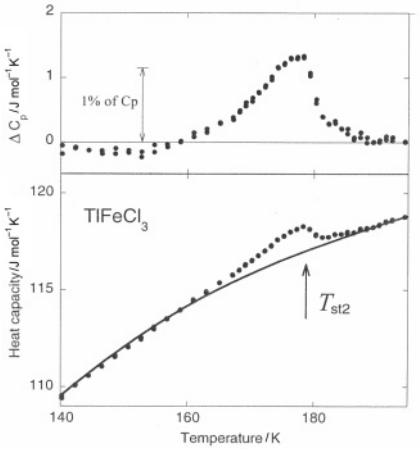

Fig. 2 The excess heat capacities for $TlFeCl_3$ around T_{st2} (as T_{N1}) due to the phase transition, which is obtained by subtracting the normal base line from the measured heat capacities. The transition is assumed experimentally as a second-order

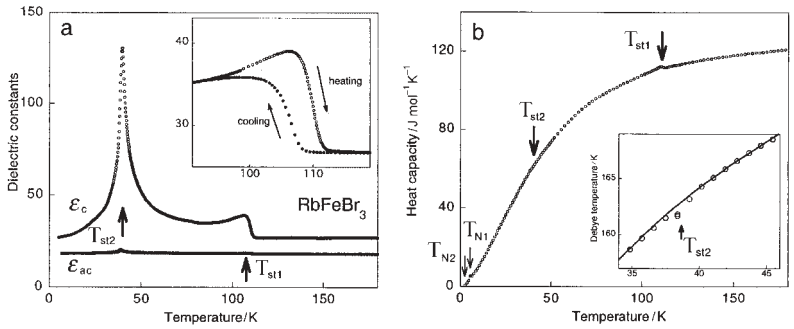

Fig. 3 The temperature dependence of dielectric constants $\varepsilon_c(T)$ and ε_{ac} (T) of $RbFeBr_3$ (Group II) at 1MHz. The inset shows the behavior of $\varepsilon_c(T)$ in cooling and heating runs in the vicinity of T_{st1} with obvious thermal hysteresis (a); The temperature dependence of molar heat capacity of $RbFeBr_3$. The inset shows the Debye characteristic temperatures corresponding to the measured heat capacities around T_{st2} (b)

The molar heat capacities measured by the relaxation method are plotted in Fig. 3b. The Debye characteristic temperatures corresponding to the measured heat capacities around T_{st2} are shown in an inset figure of Fig. 3b. The deviations from the normal base line were slightly seen at T_{st2}, where the curve of $\varepsilon_c(T)$ showed the obvious anomaly at corresponding temperatures. The first-order phase transition at T_{st1}, which class was determined by the measurement of dielectric constants, can be recognized in the normal heat capacity curve. The structural change at this temperature can be assigned that from $P6_3/mmc$ at phase I′ to $P6_3/mcm$ at phase II′.

In addition to the successive structural phase transitions, $RbFeBr_3$ also undergoes the successive magnetic phase transitions at T_{N1} (5.5 K) and T_{N2} (2.0 K) [12], though $\varepsilon_c(T)$ curve does not show any anomaly at the Néel temperatures.

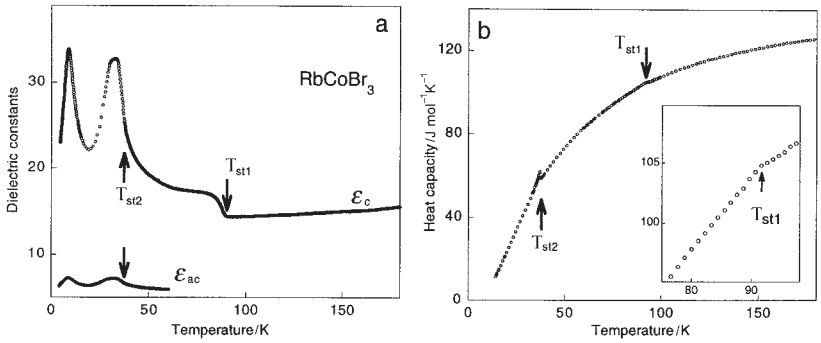

Fig. 4 The temperature dependence of dielectric constants $\varepsilon_c(T)$ and $\varepsilon_{ac}(T)$ of $RbCoBr_3$ (Group III) at 1MHz (a). The temperature dependence of molar heat capacity measurement for $RbCoBr_3$. The inset shows the detailed normal heat capacities in the vicinity of T_{st1} with a small bending (b)

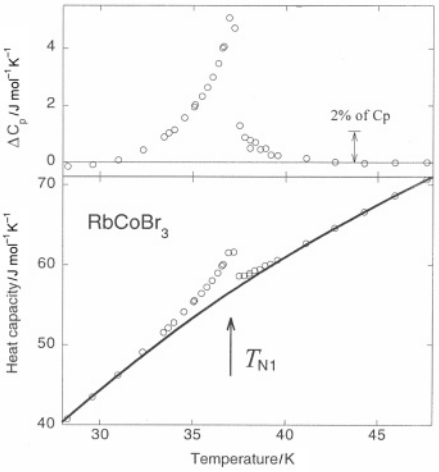

Fig. 5 The excess heat capacities for $RbCoBr_3$ around T_{st2}, which is identified with T_{N1}, due to the complex phase transitions involving magnetic and structural orders, obtained by subtracting the normal base line from the measured heat capacities. The transition is assumed experimentally as a second-order

Ferroelectricity coexists with antiferromagnetism below T_{N1}. The temperature dependence of the heat capacity around the magnetic phase transition temperatures coincide well with that previously reported by Adachi *et al.* [12].

$RbCoBr_3$ (Group III)

Figure 4a shows the temperature dependence of dielectric constants $\varepsilon_c(T)$ and $\varepsilon_{ac}(T)$ for $RbCoBr_3$, representing Group III. At a glance, peculiar two anomalies below the Néel temperature, T_{N1} is corresponding to T_{st2} for $RbCoBr_3$, are seen in $\varepsilon_c(T)$ and the corresponding peaks not necessarily small are seen in $\varepsilon_{ac}(T)$. The inflection point of $\varepsilon_c(T)$ corresponds to T_{st2} (as T_{N1}), below which a weak ferromagnetic moment grows up. The dielectric curve bends also at T_{st1}, and keeps a small value to room temperature, though a gradual increase of dielectric constant associated with the activation of impurity ionic conduction is superposed as the temperature is increased. The spontaneous polarization along the *c* axis was ascertained to appear below T_{st2} by the observations of D-E hysteresis loops and by the measurement of pyroelectric charge as a function of temperature. Judging from the presence of ferroelectricity and weak ferromagnetism, the most probable crystal structure below T_{st2} is conjectured to the polar $P6_3cm$.

The molar heat capacities measured by the adiabatic method from 13 to 200 K is plotted in Fig. 4b, where a visible hump at T_{st1} and a small bent at T_{st2} (as T_{N1}) can be seen. An excess heat capacity by subtracting the normal base line is plotted in Fig. 5. The entropy of the phase transition around T_{st2}, which is presumably second-order, should include not only the structural portion but the magnetic contributions. The baseline is estimated by fitting smoothly the data for the lower-temperature region (T<30 K) and those for the higher-temperature region (T>42 K). The molar transition entropy ΔS_m including

tail portions is estimated as 0.341 J K mol^{-1}, which is relatively small to $R\ln 2$ (5.76 J K mol^{-1}). Since the present evaluation includes both contributions of the structural and magnetic phase transitions, separation between them is desired after the construction of a thermodynamic model describing the complex transition at 37.0 K.

Summary

The properties of structural and magnetic phase transitions for three groups of '$KNiCl_3$-family' were investigated through heat capacity measurements. The specific heat anomalies are recognized at corresponding structural phase transition points of the respective compounds, though the temperature dependence of dielectric constant in every group behaves differently. Notably, the transitions between highest-temperature phase and just below one are clearly observed in every compound representing each group. However, some unidentified anomalies attributable to the impurities or imperfection of the crystal are also observed in the present measurements especially on $TlFeCl_3$ and $RbVBr_3$. Therefore, a further detailed investigation will be required for refined specimens.

References

1 M. F. Collins and O. A. Petrenko, Can. J. Phys., 75 (1997) 605.
2 D. Visser, G. C. Verschoor and D. J. W. Ijdo, Acta Cryst., B36 (1980) 28.
3 J. L. Mañes, M. J. Tello and J. M. Pérez-Mato, Phys. Rev., B26 (1986) 250.
4 K. Machida, T. Mitsui, T. Kato and K. Iio, Solid State Commun., 91 (1994) 17.
5 T. Kato, K. Machida, T. Ishii, K. Iio and T. Mitsui, Phys. Rev., B50 (1994) 13039.
6 K. Yamanaka and T. Kato, J. Phys. Soc. Jpn., 71 (2002) 1757.
7 T. Mitsui, K. Machida, T. Kato and K. Iio, J. Phys. Soc. Jpn., 63 (1994) 839.
8 K. Morishita, T. Kato, K. Iio, T. Mitsui, M. Nasui, T. Tojo and T. Atake, Ferroelectrics, 238 (2000) 105.
9 T. Mitsui, in preparation.
10 Weak moment at zero applied field of $RbFeBr_3$ below its upper antiferromagnetic ordering temperature T_{N1} (=5.5 K) was observed by the present authors: unpublished.
11 G. A. Smolenskii and I. E. Chupis, Sov. Phys. Usp., 25 (1982) 475.
12 K. Adachi, K. Takeda, F. Matsubara, M. Mekata and T. Haseda, J. Phys. Soc. Jpn., 52 (1983) 2202.